PILOT ASSISTED CHANNEL ESTIMATION FOR OFDM IN MOBILE CELLULAR SYSTEMS

Fredrik Tufvesson and Torleiv Maseng

Department of Applied Electronics, Lund University, Box 118, S-221 00 Lund, Sweden

E-mail: Fredrik.Tufvesson@tde.lth.se

Abstract — The use of pilot symbols for channel estimation introduces overhead and it is thus desirable to keep the number of pilot symbols to a minimum. The number of needed pilot symbols for a desired bit error rate and Doppler frequency is highly dependent on the pilot pattern used in orthogonal frequency division multiplexed, OFDM, systems. Five different pilot patterns are analysed by means of resulting bit error rate, which is derived from channel statistics. Rearrangement of the pilot pattern enables a reduction in the number of needed pilot symbols up to a factor 10, still retaining the same performance. The analysis is general and can be used for performance analysis and design of pilot patterns for any OFDM system.

I. INTRODUCTION

The mobile channel introduces multipath distortion of the signalling waveforms. Both the amplitude and phase are corrupted and the channel characteristics changes because of movements of the mobile. In order to perform coherent detection, reliable channel estimates are required. These can be obtained by occasionally transmitting known data or so called "pilot symbols". The receiver interpolates the channel information derived from the pilots to obtain the channel estimate for the data signal, see Fig. 1.

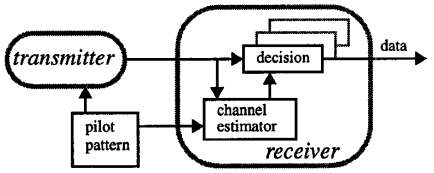

Fig. 1 The pilot pattern is known both by the receiver and the transmitter. The purpose is to minimize the number of transmitted pilot symbols without increasing the bit error rate.

OFDM, orthogonal frequency division multiplexing, is used and proposed for several broadcast systems and there is a growing interest in using the technique for the next generation land mobile communication system. In OFDM systems the information signal can be seen as divided and transmitted by several narrowband sub-carriers. Typically, for practical OFDM systems, the frequency spacing is less than the coherence bandwidth and the symbol time is less than the coherence time. This means that a receiver and pilot estimation pattern that take advantage of the relatively large coherence bandwidth and coherence time can manage with less pilot symbols, thereby minimizing the overhead introduced by the pilot symbols. The problem is to decide where and how often to insert pilot symbols. The spacing between the pilot symbols shall be chosen small enough to enable reliable channel estimates but large enough not to increase the overhead too much. This paper includes among all an algorithm of how to design a suitable pilot estimation pattern.

In a multicarrier system there exist a unique opportunity to determine various parts of the channel impulse response, as opposed to a single-carrier system. It is no use to make efforts to determine already known parts. Until now it seems like no one has looked into the impact of the placement of the pilot symbols for multicarrier systems. Cavers [5] made an exhaustive theoretical analysis for single-carrier systems. He pointed out that it was appropriate that 14% of the sent symbols were pilot symbols to be able to handle large Doppler values ($f_dT_s=0.05$). Some pilot estimation patterns for OFDM has been presented in the literature, see e.g. [6], [7]. Comparisons between these and the one proposed here are shown later.

II. ESTIMATION STRATEGIES

Five different pilot patterns are analyzed, see Fig. 2.

1. Measure all channels at the same time, compare to a broadband single-carrier system.
2. Measure the channels in increasing order, one at a time.
3. Measure the channels one at a time in a smart, but predetermined, way. The measurement order is derived upon channel statistics and is optimal in the sense that the total bit error rate is kept at a minimum each symbol time.
4. A pilot pattern presented by T. Mueller *et al.* [6], where the pilots are located with equidistant spacings in time and frequency.
5. A pilot pattern by P. Hoeher [7], used in [4]. The pilot symbol locations are shifted one step in frequency each pilot interval.

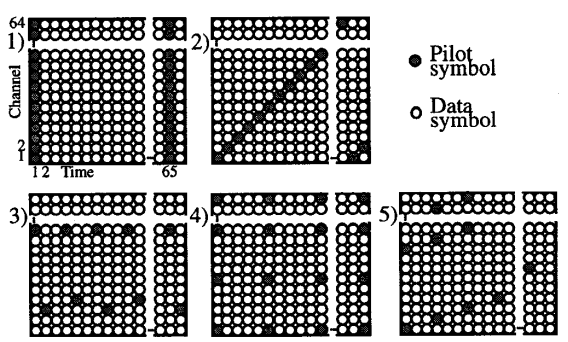

Fig. 2 Examples of pilot patterns analyzed.

0-7803-3659-3/97 $10.00 ©1997 IEEE

Authorized licensed use limited to: Sterne Kessler Goldstein Fox. Downloaded on August 04,2022 at 18:29:02 UTC from IEEE Xplore. Restrictions apply.

For comparison the same amount of pilots is used, one of 64 sent symbols. This means that only 1.6% extra overhead is introduced by the pilots, but this is not sufficient for large Doppler frequencies in some of the cases.

III. SYSTEM

At different signal to noise ratios the resulting bit error rate from each pilot pattern is evaluated using the algorithms given in Section VIII. A matched filter receiver and coherent BPSK or QPSK are used. Additive white Gaussian noise is assumed for every sub-channel. The channel has delays and Rayleigh distributed amplitudes according to the COST 207: "Typical Urban profile". The complex parts of the transfer function are assumed to change according to a first order auto-regressive process as described in Section VI. The reason for using this model is to get a linear system which rather easy can be handled algebraically. A Kalman filter is used to estimate the frequency response of the channel. From the filter, a time dependent covariance matrix is given as described in Section VII. This is used to calculate the expected bit error rate for each channel. See Fig. 3 for a description of the system.

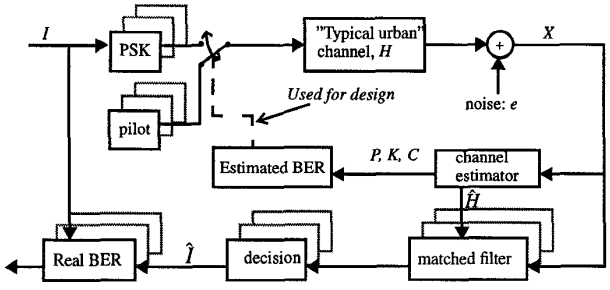

Fig. 3 Overview of the system used to analyze the estimation patterns.

IV. RESULTS

The resulting bit error rate curves of the pilot patterns are presented for different Doppler frequencies in Fig. 4.

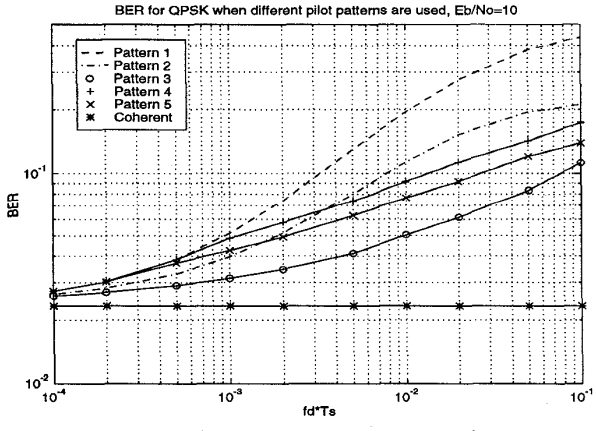

Fig. 4 Resulting bit error rate as a function of Doppler value when the different pilot patterns are used. The same number of pilot symbols are used for all curves.

For a given Doppler frequency the pilot pattern used sets the limit for the lowest pilot density to be used, alternatively for a given pilot density it limits the maximum Doppler frequency allowed. The calculations are made at 1800 MHz using 10 kHz channel separation between 64 OFDM channels carrying in total 640 ksymbols/s. No intersymbol interference, perfect synchronization and known Doppler frequency, f_d, is assumed. 1.6% of the sent symbols are pilot symbols and the average bit error rate of the 64 channels is presented.

The bit error rate is degraded both by imperfect channel estimates and noise disturbances. The pilot pattern used determines the conversion between noise limited and estimate limited region, see Fig. 5.

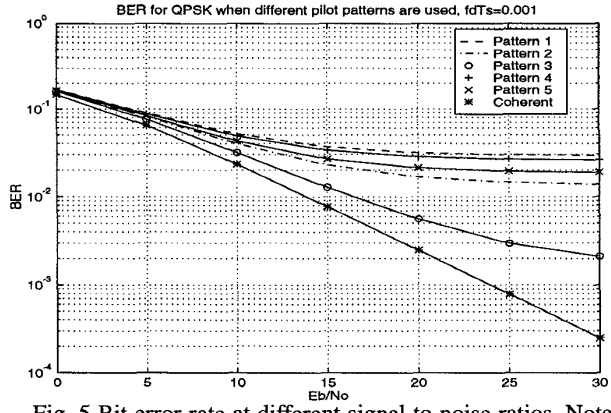

Fig. 5 Bit error rate at different signal to noise ratios. Note the difference between the error floors.

It is interesting to study the resulting pattern when estimating the channel that gives the lowest bit error rate (strategy 3). A steady state pilot pattern is often achieved where only few of the sub-channels are measured, see Fig. 6. Channel estimates of the other sub-channels are achieved by filtering.

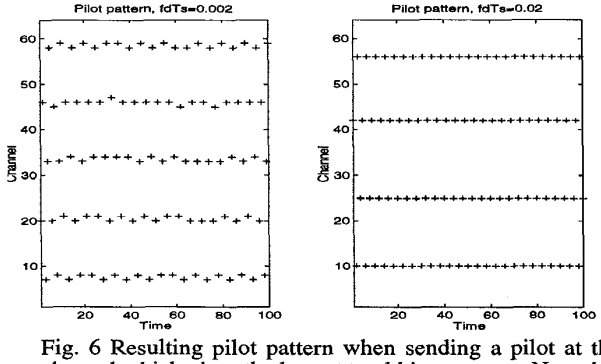

Fig. 6 Resulting pilot pattern when sending a pilot at the channel which gives the lowest total bit error rate. Note that only few channels will be used for pilot symbols.

To see the effect of mismatch between the pilot pattern design parameters and the actual parameters, the optimal pilot patterns (pattern 3) for three Doppler values were used when moving at another speed. The actual Doppler frequency was as before assumed to be known by the estimator, just to see the effect of the pilot pattern without influences of the estimation algorithm. The designed pilot patterns for the "typical urban" environment were also used in "hilly terrain" and "rural area"

Authorized licensed use limited to: Sterne Kessler Goldstein Fox. Downloaded on August 04,2022 at 18:29:02 UTC from IEEE Xplore. Restrictions apply.

specified in [2] to see the influence of the propagation environment on the bit error rate, see Fig. 7.

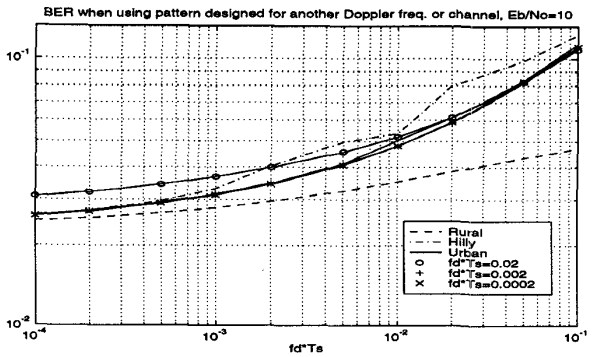

Fig. 7 Changes in the bit error rate due to Doppler mismatch and power delay profile mismatch. The pilot patterns designed for f_dT_s=*0.02, 0.002* and *0.0002* were used at different Doppler values and the designed patterns for typical urban environment were used in hilly terrain and rural area.

As seen in the figure, the pilot patterns are robust to mismatches in the design parameters.

V. DISCUSSION

To minimize the bit error rate it is desirable to spread the pilot symbols both in time and in frequency, as seen in Fig. 4 and Fig. 5. Normally a worst case design is made for the channel estimation system and then we suggest to tailor the pilot pattern to each base station site. A suitable pilot pattern can be calculated once the propagation environment and maximum expected speed in the particular cell is known. In such a system, the pilot pattern used in the cell is among the information transferred to the mobile when it logs into a new cell. When designing the pilot pattern one also has to take the estimation algorithm into account. Here the estimation algorithm is used only for evaluation and the complexity of the used algorithm is not a problem. In some cases the pilot pattern has to aid the estimation algorithm to enable a less complex one. The estimation algorithm used here, the Kalman filter based on an AR-process, has no delay and the received signal can be detected immediately, i.e. no future pilot symbols is taken into account when making the channel estimate. If the received signal is stored in a memory, the pilot symbols can be used in both "time directions" and the time spacings between pilot symbols can be increased, retaining the same performance.

The degradation due to mismatch in design parameters is mainly caused by the estimation algorithm and therefore the curves for different Doppler values do not differ much. When the pilot pattern is designed for higher Doppler values than the actual one, an increased error rate is achieved since the pilot symbols are not located as close to each other in frequency as desired. In rural area the bit error rate becomes lower due to the increased frequency correlation while the opposite happens in hilly terrain. In the first case, an even better result is achieved with less pilots along the frequency axes and more along the time axes.

The bit error rates within the sub-channels differ depending on where the pilots are located. When minimizing the total bit error rate (pattern 3) the channels of the sides get higher error rate, see example in Fig. 8.

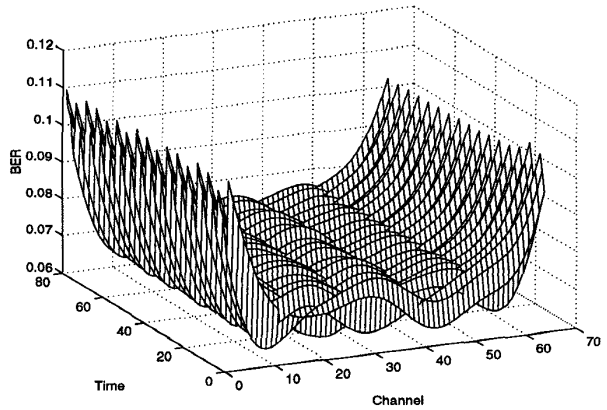

Fig. 8 The bit error rate becomes higher for the side channels when the total bit error rate is kept at a minimum

VI. CHANNEL MODEL

The time dependent impulse response, $h(\tau, t)$, is assumed to be a sum of reflections, see (1) where $\delta(t)$ denotes the dirac-function.

$$h(\tau, t) = \sum_{n=1}^{N} a_n(t) \cdot \delta(t - \tau_n) \tag{1}$$

The tap coefficients, $a_n(t)$, and the tap delays, τ_n, are chosen according to the COST 207 "Typical Urban" model in the GSM specification [2]. The transfer functions, $H(f,t)$, are obtained by the Fourier transform and these are the functions we want to estimate for the different carriers. These channel transfer functions are regarded as flat fading and constant during a symbol time.

A first order AR-process is used to model how the different taps may change from one time instant to another. If we look at all the transfer functions at the same time, it is possible to set up a state-space model of the form:

$$\begin{aligned} H(k+1) &= \phi H(k) + v(k) \\ y(k) &= C(k)H(k) + e(k) \end{aligned} \tag{2}$$

The matrix ϕ is a diagonal N*N-matrix (here treated as a scalar) with elements

$$e^{-k_{AR} 2\pi f_d T_s} \tag{3}$$

that define the AR-process. T_s is the symbol time including any cyclic prefix or guard space. The white noise $v(k)$ has covariance matrix $R_1 = F \cdot R_{GSM} \cdot F^*$, where R_{GSM} corresponds to the multipath intensity profile described in [2]. The vector $y(k)$ is the measured transfer functions. $C(k)$ is an observation vector with ones only at the positions (channels) measured at time KT_s and $e(k)$ is measurement noise with a diagonal covariance matrix R_2.

The parameter k_{AR} in the auto-regressive process for the channel changes is chosen to adjust the "memory" so that it

Authorized licensed use limited to: Sterne Kessler Goldstein Fox. Downloaded on August 04,2022 at 18:29:02 UTC from IEEE Xplore. Restrictions apply.

corresponds to the "memory" of Jakes' model. Channels corresponding to the U-shaped spectrum given in [8] were simulated and then estimators based on an AR-model with different k_{AR} were used, see Fig. 9

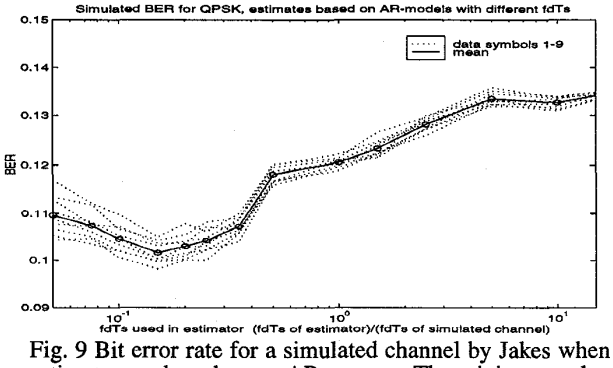

Fig. 9 Bit error rate for a simulated channel by Jakes when estimates are based on an AR-process. The minimum value is reached for $k_{AR}=0.15$.

Simulations were performed with one sub-channel ($E_b/N_o= 10$, $f_dT_s=0.002$) with every tenth symbol as a pilot symbol. In the figure the bit error rates of the nine data symbols are shown. Fig. 9 shows that the best fit, in this case, is reached for $k_{AR}\approx 0.15$.

The adjustment of the AR-process can also be seen as an adjustment of the bandwidth. If we set the 90% power bandwidth of the AR process equal to the bandwidth of the Doppler spread, see Fig. 10, a value of $k_{AR}\approx 0.158$ can be calculated. This is the value used for all bit error rate calculations throughout the paper.

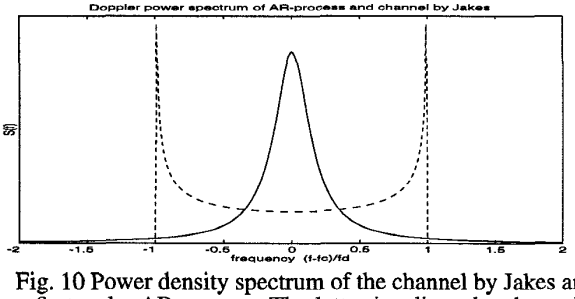

Fig. 10 Power density spectrum of the channel by Jakes and a first order AR-process. The latter is adjusted to have the 90% power bandwidth equal to the Doppler spread.

VII. CHANNEL ESTIMATOR

For the analysis and pilot pattern design a Kalman filter is used to estimate the transfer functions. The Kalman filter is causal and uses measurements up to time k to estimate the transfer functions, $H(k)$. The Kalman filter is given [3] by (4)-(8), where X^* denotes conjugate transpose of X:

$$\hat{H}(k|k) = \hat{H}(k|k-1) + P(k|k-1)C(k)^* \cdot \{C(k)P(k|k-1)C(k)^* + R_2\}^{-1}(y(k) - C(k)\hat{H}(k|k-1)) \tag{4}$$

$$\hat{H}(k+1|k) = \phi\hat{H}(k|k-1) + K(k)[y(k) - C(k)\hat{H}(k|k-1)] = \phi\hat{H}(k|k) \tag{5}$$

$$K(k) = \phi P(k|k-1)C(k)^* \cdot [C(k)P(k|k-1)C(k)^* + R_2]^{-1} \tag{6}$$

$$P(k+1|k) = \phi P(k|k-1)\phi^* + R_1 - K(k)[C(k)P(k|k-1)C(k)^* + R_2]K(k)^* \tag{7}$$

$$P(k|k) = P(k|k-1) - P(k|k-1)C(k)^* \cdot [C(k)P(k|k-1)C(k)^* + R_2]^{-1}C(k)P(k|k-1) \tag{8}$$

The reconstruction error $\tilde{H}(k|k) = H(k) - \hat{H}(k|k)$ is given by:

$$\tilde{H}(k|k) = [\phi - K(k)C(k)]\tilde{H}(k-1|k-1) + v(k-1) - P(k|k-1)C(k)^*[C(k)P(k|k-1)C(k)^* + R_2]^{-1} \cdot \{e(k) + C(k)v(k-1)\} \tag{9}$$

The Kalman filter is optimal in the sense that the variance of the reconstruction error is minimized. The matrix $P(k|k)$ is the variance matrix and this is used together with K to make an estimate of the bit error rate, which in turn is used to decide the order in which the channels are going to be measured. For pattern 3, the channel is chosen that minimizes the total bit error rate of the channels after the measurement. The matrices $P(k|k)$ and K are independent of the measured values and therefore it is possible to precompute the order in which the channels are going to be measured.

VIII. BIT ERROR RATE CALCULATIONS

The bit error rate is calculated for BPSK and QPSK. A matched filter receiver is assumed. The sampled output of this filter is given by

$$X_m = 2\varepsilon H_m e^{j\frac{2\pi}{M}(n-1)} + e_m \tag{10}$$

where ε is the signal energy, H_m is the current transfer function at channel m, n is the signal alternative among M sent and e_m is white gaussian noise. The bit error rate at channel m is calculated as [1]

$$P_{bmBPSK} = \frac{1}{2}(1-\mu_m)$$
$$P_{bmQPSK} = \frac{1}{2}\left(1 - \frac{\mu_m}{\sqrt{2-\mu_m^2}}\right) \tag{11}$$

where

$$\mu_m = \frac{E[X_m\hat{H}_m^*]}{\sqrt{E[|X_m|^2]E[|\hat{H}_m|^2]}} \tag{12}$$

$\hat{H}_m$ are the outputs of the Kalman filter. These are not known in advance and therefore (13) - (15) are used. If matrix notation is used and signal alternative 1 is used for the pilot symbol (does affect the analysis here, but in practise different pilot symbol alternatives should be used), the expectations for all the channels can be calculated as:

Authorized licensed use limited to: Sterne Kessler Goldstein Fox. Downloaded on August 04,2022 at 18:29:02 UTC from IEEE Xplore. Restrictions apply.

$$E[X(k)\hat{H}(k)^*] \quad (13)$$
$$= E[\{2\varepsilon H(k) + N(k)\}\{H(k) - \tilde{H}(k)\}^*]$$
$$= 2\varepsilon E[H(k)H(k)^*] - 2\varepsilon E[H(k)\tilde{H}(k)^*]$$

$$E[|X(k)|^2] = E[\{2\varepsilon H(k) + N(k)\}\{2\varepsilon H(k) + N(k)\}^*] \quad (14)$$
$$= 4\varepsilon^2 E[H(k)H(k)^*] + E[N(k)N(k)^*]$$

$$E[|\hat{H}(k)|^2] = E[\{H(k) - \tilde{H}(k)\}\{H(k) - \tilde{H}(k)\}^*] \quad (15)$$
$$= E[H(k)H(k)^*] - 2E[H(k)\tilde{H}(k)^*] + E[\tilde{H}(k)\tilde{H}(k|k)^*]$$

The expected values $E[X(k)\hat{H}(k)^*]$, $E[|X(k)|^2]$ and $E[|\hat{H}(k)|^2]$ are independent of the measured values but dependent upon which channels that are measured. Therefore they are time dependent. The expectations can be calculated as:

$$E[H(k)H(k)^*] \quad (16)$$
$$= E[\{\phi H(k-1) + v(k-1)\}\{\phi H(k-1) + v(k-1)\}^*]$$
$$= \phi^2 E[H(k-1)H(k-1)^*] + E[v(k-1)v(k-1)^*]$$
$$= R_1/(1-\phi^2)$$

$$E[N(k)N(k)^*] = R_2 \quad (17)$$

$$E[H(k)\tilde{H}(k|k)^*] = E[H(k)H(k)^* - H(k)\hat{H}(k|k)^*] \quad (18)$$
$$= E[\phi H(k-1)\tilde{H}(k-1)^*\phi^* + R_1 - R_1 C(k)^* a^*$$
$$- \phi H(k-1)\tilde{H}(k-1)^*\phi^* C(k)^* a^*]$$
$$= (\phi E[H(k-1)\tilde{H}(k-1)^*]\phi^* + R_1)(I - C(k)^* a^*)$$

where

$$E[\tilde{H}(k|k)\tilde{H}(k|k)^*] = P(k|k) \quad (19)$$

$$a = P(k|k-1)C(k)^*\{C(k)P(k|k-1)C(k)^* + R_2\}^{-1} \quad (20)$$

The bit error rate calculation is compared and verified by simulations. Proakis [1] gives expressions for the bit error rate when estimating a constant Rayleigh channel using different numbers of pilot symbols, see Fig. 11.

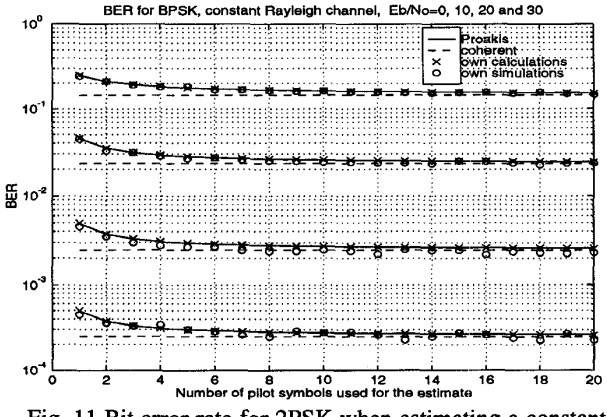

Fig. 11 Bit error rate for 2PSK when estimating a constant Rayleigh channel with several pilot symbols at different signal to noise ratios.

The bit error rate when using only one pilot symbol corresponds to estimating a rapidly changing channel or the first estimate of an unknown channel. Then, only the latest measurement is useful. In a similar way, the bit error rate when estimating a constant channel with use of (infinitely) many pilot symbols corresponds to that of coherent detection. Normally in a practical system the effect of the estimation is somewhere between these two cases.

IX. CONCLUSIONS

The bit error rate for pilot assisted QPSK modulation is calculated when using different pilot patterns. The ability to estimate the channel reliably when it changes due to e.g. vehicle movements is highly dependent on the pilot pattern used. By rearranging the pilot pattern it is, in some cases, possible to handle 10 times higher Doppler frequency alternatively possible to reduce the number of needed pilot symbols the same amount, still retaining the same bit error rate. Alternatively the new pilot pattern could be used to reduce the bit error rate up to a factor 5, even more in a low noise environment. The pilot symbols in the proposed pilot pattern are spread out both in time and frequency. For a given propagation environment, e.g. a base station site, it is possible to pre-calculate a suitable pilot pattern.

REFERENCES

[1] J. G .Proakis, Digital Communications, third edition, McGraw-Hill, USA, 1995.

[2] European Telecommunications Standard Institute, GSM 05.05, version 4.6.0, July 1993.

[3] J. M. Mendel, Lessons in Estimation Theory for Signal Processing, Communications and Control, Prentice-Hall, USA, 1995.

[4] M. Sandell, Design and Analysis of Estimators for Multicarrier Modulation and Ultrasonic Imaging, Ph.D. thesis, Luleå University of Technology, Sweden, 1996.

[5] J. K. Cavers, An Analysis of Pilot Symbol Assisted Modulation for Rayleigh Fading Channels, IEEE Trans. Vehic. Tech. vol 40, no 4, pp 686-693, nov 1991.

[6] T. Mueller, K. Brueninghaus and H. Rohling, Performance of Coherent OFDM-CDMA for Broadband Mobile Communications, Wireless Personal Communications 2, pp 295-305, Kluwer, Netherlands, 1996.

[7] P. Hoeher. TCM on Frequency-Selective Land-Mobile Fading Channels, Proc. of 5th Tirrenia Int. Workshop in Dig. Communications, Tirrenia, Italy, Sept. 1991.

[8] W. Jakes, Microwave Mobile Communications, Wiley-Interscience, USA 1974

Authorized licensed use limited to: Sterne Kessler Goldstein Fox. Downloaded on August 04,2022 at 18:29:02 UTC from IEEE Xplore. Restrictions apply.